Journal of Marine Science and Application (2018) 17:564–577
https://doi.org/10.1007/s11804-018-00056-4

RESEARCH ARTICLE

Effect of a Submerged Porous Plate on the Hydroelastic Response of a Very Large Floating Structure

Harekrushna Behera[1] · Trilochan Sahoo[2] · Chiu-On Ng[3]

Received: 23 August 2017 / Accepted: 30 April 2018 / Published online: 5 December 2018

Abstract

Scattering of oblique flexural-gravity waves by a submerged porous plate in a finite water depth is investigated under the assumptions of linearized surface waves and small-amplitude structural response. The study is carried out using eigenfunction expansions and the corresponding orthogonal mode-coupling relations associated with flexural-gravity waves in uniform water depth. The characteristics of the roots of the complex dispersion relation are examined using the principle of counting argument and contour plot. Characteristics of the flexural-gravity waves are studied by assuming both the floating elastic plate and the submerged porous plate are infinitely extended in horizontal directions. The effectiveness of the submerged porous structure on the reflection, transmission, and dissipation coefficients is analyzed for various wave and structural parameters.

Keywords Flexural-gravity wave · Mode-coupling relation · Dispersion relation · Porous plate · Reflection and transmission coefficients

1 Introduction

Over the past two decades, coastal engineering has seen a growing interest in wave–structure interaction as demanded by the need for the attenuation of waves in order to create a tranquil nearshore zone. Compared with vertical structures, which tend to block current and are subject to large wave loading, the use of submerged horizontal structures as a breakwater is more preferable as these structures do not hamper the seascape and does not block the incoming waves. The interaction of surface waves with a submerged structure may result in a phase shift of the waves, which may then lead to a destructive interference of the incoming and reflected waves. Moreover, structural porosity helps in dissipating the wave energy. Although interaction between surface waves and a submerged plate was studied as early as Heins (1950), an effective use of submerged structures as a breakwater in a coastal setting was not studied until Ijima et al. (1970). A detailed review on the performance of submerged horizontal plates for wave control can be found in Yu (2002).

A model for a wave absorbing system, developed by Cho and Kim (1998), involved an inclined submerged horizontal perforated plate and a vertical wall. Their mathematical model was formulated based on the linearized wave theory and Darcy's law for flow past porous structures. They validated their theoretical and computational results through full-scale experiments. Liu and Li (2011) analyzed interaction of surface gravity waves with an offshore submerged horizontal porous-plate by means of the matched eigenfunction-expansion method. Evans and Peter (2011) studied the interaction of surface gravity waves with a submerged semi-infinite porous plate via the Wiener-Hopf technique, and a finite porous plate via the residue technique. Hu and Wang (2005) studied wave past a system consisting of a submerged horizontal plate and a vertical porous wall, and demonstrated that, for a suitable configuration, the system can reduce wave transmission effectively. More studies on wave interaction with a suitable arrangement of submerged porous plates can be found in Liu et al. (2007) and the references cited therein. Apart from wave interaction with submerged structures, an extensive work has been done on wave interaction with submerged flexible

✉ Harekrushna Behera
hkb.math@gmail.com

[1] SRM Research Institute and Department of Mathematics, SRM Institute of Science and Technology, Kattankulathur 603203, Tamil Nadu, India

[2] Department of Ocean Engineering and Naval Architecture, Indian Institute of Technology, Kharagpur 721302, India

[3] Department of Mechanical Engineering, The University of Hong Kong, Pokfulam, Hong Kong, China

porous structures. These types of structures are very light in weight and cost-effective. Apart from energy loss by structural porosity, wave energy can also be dissipated through structural deformation, which will attenuate both the incident and scattered waves. Cho and Kim (1998) investigated oblique wave interaction with a submerged horizontal flexible membrane using the boundary element method and eigenfunction expansion method. The work was later extended by Cho and Kim (2000) to wave diffraction by a submerged porous flexible membrane. In both studies, the analytical and numerical results were supported by experimental validations. On the other hand, Hassan et al. (2009) analyzed the surface wave interaction with submerged flexible plates of finite and semi-infinite lengths by combining the dynamic and kinematic conditions on the submerged plate. In this approach, the physical problem was converted into a boundary value problem associated with Laplace equations satisfying certain high-order conditions on the structural boundary. Williams and Meylan (2012) investigated the surface wave interaction with a semi-infinite submerged elastic plate using the Wiener-Hopf technique. Recently, Behera and Sahoo (2015) looked into the hydroelastic analysis of surface gravity wave interaction with a submerged flexible porous plate in finite water depth. Meylan et al. (2017) studied scattering of surface waves by a floating porous elastic plate in three dimensions using coupled boundary element and finite element method to account for plates of arbitrary configurations. Behera and Ng (2017) investigated oblique wave scattering by a system of floating and submerged porous elastic plates. Recently, Koley and Sahoo (2017) analyzed oblique wave scattering by a floating flexible porous membrane by converting the boundary value problem into pairs of Fredholm integral equations in terms of the velocity potentials and their normal derivatives along the membrane.

Recently, significant progress has been made on the interaction of surface gravity waves with very large floating structures for ocean space utilization. Hydroelastic analysis of these structures has been performed for understanding the performance of these large-scale structures under the action of waves. Wang and Tay (2011) reviewed various applications, research, and development of VLFS over two decades. A parallel branch of study is the interaction of surface gravity waves with floating ice sheet where the floating ice sheet is modeled as an elastic plate and a state-of-the-art research on wave–ice interaction can be found in Squire (2011). Various two-dimensional investigations have been generalized to study wave interaction with floating structures in three-dimensions. Mondal et al. (2013) studied the wave-structure interaction problems in three-dimensions in case of homogeneous fluids having a plate covered surface which was generalized by Mondal and Sahoo (2012, 2014) to deal with such problems in cases of stratified fluids in two-layer and three-layer fluid systems assuming the presence of plate covered surface and interfaces. Mandal et al. (2017) studied various characteristics of eigen-systems for flexural-gravity waves which is generated due to the interaction of surface gravity waves with large flexible floating structures. For mitigating the hydroelastic response of the very large floating structures in waves, several methods have been proposed and a review on the same can be found in Wang et al. (2010) and Tavana and Khanjani (2013). Ohta et al. (1999) investigated the effect of submerged vertical as well as horizontal plate attached at the fore end of the VLFS. Watanabe et al. (2003) examined the effect of attached horizontal plates to VLFS. Cheng et al. (2015) analyzed the hydroelastic response on a very large floating structure edged with a pair of submerged horizontal plates. Recently, Cheng et al. (2016) analyzed the role of dual inclined perforated plates for mitigating hydroelastic response of a VLFS using hybrid finite element-boundary element method. It may be noted that in case of rigid submerged plates, no edge conditions are prescribed as a part of the boundary value problem for uniqueness of the solution unlike the case of a flexible submerged plate in spite of the fact that the plates are kept in position with appropriate supporting system. Recently, Mohapatra and Sahoo (2014a) analyzed gravity wave interaction with floating and submerged elastic plate system in two-dimensions, which was generalized by Mohapatra and Sahoo (2014b) to study oblique surface wave interaction with a floating elastic plate in the presence of a flexible submerged plate. Moreover, three-dimensional hydroelasticity theory is used to predict the hydroelastic response of flexible floating interconnected structures. Effective use of hinges or semi-rigid connectors for reducing hydroelastic responses of VLFS have been studied by Fu et al. (2007). Recently, Yoon et al. (2014) performed hydroelastic analysis of floating plates with multiple hinge connections in regular waves. Using Biot's consolidation theory, Das et al. (2016) studied the effect of poroelastic bed on flexural-gravity wave motion in a single- or two-layer fluid. Recently, Das and Sahoo (2017) studied the effect of viscoelastic bed on the hydroelastic response of a very large floating structure.

Meanwhile, significant progress has also been made on scattering of flexural-gravity wave by vertical barriers for reducing structural vibration of the large floating elastic structure. Takagi et al. (2000) proposed a simple anti-motion device, which a box-shaped body is attached to an edge of the floating structure. The performance of this device was investigated theoretically and experimentally. The theory was based on the eigenfunction expansion method. Chakrabarti et al. (2003) investigated a class of such surface water wave problems, involving the vertical barrier, under the assumption that there exists a thin ice-cover on the surface of the deep water. Using the method of multipoles, Das and Mandal (2009) studied wave scattering by a circular cylinder half-immersed in water with an ice-cover. Later, Maiti and Mandal (2010) used the hyper singular integral equation method for flexural-gravity wave interaction with an inclined submerged vertical barrier. Recently, Manam and Kaligatla (2011) provided an explicit solution to study the scattering of flexural-gravity waves by a rigid vertical barrier. However, to the author's knowledge, no study has been performed in the literature to understand the role played by a submerged permeable horizontal structure in attenuating the structural response of a large floating structure/ice sheet.

The present study aims to look into the effect of a submerged porous plate on the mitigation of hydroelastic response of a very large floating structure. In terms of three-dimensional Cartesian coordinates, a model is developed for the interaction between waves and a very large floating structure, under the conditions of linearized water waves and small-amplitude structural response. Moreover, Darcy law is used to describe waves propagating past a submerged porous structure as in Cho and Kim (2013). Moreover, since the submerged porous plate is assumed to be rigid in nature, no edge conditions are prescribed near the submerged plate edges at the edges in spite of the fact that the submerged plate is kept is position with appropriate support system. Moreover, since emphasis is given to understand the effect of the submerged porous plate on the hydroelastic response analysis of the floating plate, role of support system which keep the structure in position is not taken into consideration in the present study. Here, it is assumed that the floating elastic plate is infinitely extended both lengthwise and spanwise, while the submerged porous plate can be of finite length and infinitely large spanwise. In the limiting case where the submerged plate is also infinitely extended both lengthwise and spanwise, its effect on the phase velocity of the flexural-gravity waves and floating plate deflection is examined in detail. It may be noted that the length of the floating elastic plate is assumed to be very large compared to the length of the submerged porous plate. Thus, for mathematical simplicity, the floating plate is assumed to be infinitely extended. For flexural gravity wave scattering by a finite submerged porous plate, the physical problem is handled using the eigenfunction expansion method and mode-coupling relation. Results are generated to reveal the effect of various physical properties (porosity of the submerged porous plate, rigidity and compressive force of the very large floating plate, and wave incident angle) on the wave reflection and transmission, and dissipation.

2 Mathematical Formulation

In this section, the problem of oblique flexural-gravity waves scattered by a submerged horizontal finite porous plate is mathematically formulated. A definition sketch of the problem is shown in Fig. 1. We introduce a three-dimensional Cartesian coordinate system, wherein the $x-y$ plane is a horizontal plane and the z−axis is taken vertically downward into

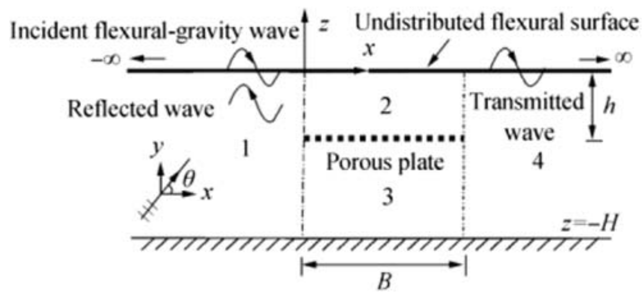

Fig. 1 Schematic diagram of flexural-gravity waves scattered by a submerged finite horizontal porous plate

the fluid region. It is assumed that an infinite ice-sheet or elastic plate of small thickness d floats on the undisturbed water surface z=0, and a finite submerged thin porous plate of length B is kept horizontally at $z = -h$ in water of finite depth H, as shown in Fig. 1.

The whole fluid domain is decomposed into four regions: region 1, 2, 3, and 4. It is assumed that the fluid is inviscid, incompressible, and the motion is irrotational. Thus, the velocity potentials $\Phi_j(x, y, z, t)$ for $j = 1, 2, 3, 4$ satisfy the three-dimensional Laplace equation as given by

$$\left(\frac{\partial^2}{\partial x^2}+\frac{\partial^2}{\partial z^2}+\frac{\partial^2}{\partial z^2}\right)\Phi_j = 0\,, \quad \text{for} \quad j = 1,2,3,4 \tag{1}$$

Assuming that the bottom bed is rigid, the bottom boundary condition is given by

$$\frac{\partial \Phi_j}{\partial z} = 0 \quad \text{on}\, z = -H, \quad \text{for} \quad j = 1,3,4 \tag{2}$$

The linearized kinematic condition on the plate covered surface at z=0 is given by

$$\frac{\partial \Phi_j}{\partial z} = \frac{\partial \eta}{\partial t}, \quad \text{for} \quad j = 1,2,4 \tag{3}$$

where η is the deflection of the floating elastic plate. The linearized hydrodynamic pressure in the j-th region is given by

$$P_j = -\rho\left(\frac{\partial \Phi_j}{\partial t} - gz\right) \tag{4}$$

where ρ is the density of water and g is the acceleration due to gravity. The thin elastic plate equation in the presence of uniform compressive force T_c, which is floating on the mean free surface of water along the $x-y$ plane at z=0, is given by

$$\left(EI\nabla^4_{xy} + T_c\nabla^2_{xy} + \rho_e d\frac{\partial^2}{\partial t^2}\right)\eta = -P_j(x,y,z,t) \quad \text{for} \quad j = 1,2,4 \tag{5}$$

where $\nabla_{xy}^2 = \partial^2/\partial x^2 + \partial^2/\partial y^2$, and E, d and ρ_e are the Young's modulus, thickness, density of the elastic plate, respectively with $I = d^3/[12(1-\nu^2)]$ and ν is the Poisson's ratio of the elastic plate. Eliminating P_j and η, from Eqs. (4) and (5), the linearized condition on the plate covered surface is obtained as

$$\left(EI\nabla_{xy}^2 + T_c\nabla_{xy}^2 + \rho_e d\frac{\partial^2}{\partial t^2}\right)\frac{\partial \Phi_j}{\partial z} = \rho\left(\frac{\partial^2 \Phi_j}{\partial t^2} - g\frac{\partial \Phi_j}{\partial z}\right) \quad \text{on } z = 0\text{, for } j = 1, 2, 4 \tag{6}$$

Assuming that the flexural-gravity wave is propagating by making an oblique angle θ with the x–axis and the wave motion is simple harmonic in time with angular frequency ω, the velocity potentials and plate deflection are written in the forms $\Phi_j(x, y, z, t) = \mathrm{Re}\left\{\phi_j(x, z)e^{-i(\mu_y y - \omega t)}\right\}$ for $j = 1, 2, 3, 4$ and $\eta(x, y, t) = \mathrm{Re}\left\{\zeta(x)e^{-i(\mu_y y - \omega t)}\right\}$ with $\mu_y = k_0 \sin\theta$ and k_0 being the wave number of the incident wave. Thus, the spatial velocity potentials $\phi_j(x, z)$ for $j = 1, 2, 3, 4$ satisfy the Helmholtz equation which is given by

$$\left(\frac{\partial^2}{\partial x^2} + \frac{\partial^2}{\partial z^2} - \mu_y^2\right)\phi_j = 0\text{, for } j = 1, 2, 3, 4 \tag{7}$$

along with the rigid bottom boundary condition

$$\frac{\partial \phi_j}{\partial z} = 0, \text{ on } z = -H \tag{8}$$

The linearized kinematic boundary condition on the floating elastic plate is given by

$$\left(D\frac{\partial^4}{\partial z^4} - Q\frac{\partial^2}{\partial z^2} + 1\right)\frac{\partial \phi_j}{\partial z} + K\phi_j = 0 \tag{9}$$

where j=1,2,4, $D = EI/(\rho g - m_s\omega^2)$, $Q = T_c/(\rho g - m_s\omega^2)$, $K = \rho\omega^2/(\rho g - m_s\omega^2)$, $m_s = \rho_e d$. The continuity of pressure and velocity at x=0 and $x = B$ yield

$$\phi_j = \begin{cases} \phi_2, \\ \phi_3, \end{cases} \quad \text{and} \quad \frac{\partial \phi_j}{\partial x} = \begin{cases} \dfrac{\partial \phi_2}{\partial x} \\ \dfrac{\partial \phi_3}{\partial x} \end{cases} \tag{10}$$

where j=1 at x=0 and j=4 at $x = B$. The boundary condition on the submerged porous plate is given by, as in Cho and Kim (2013),

$$\frac{\partial \phi_2}{\partial z} = \frac{\partial \phi_3}{\partial z} = i\sigma(\phi_3 - \phi_2), \text{on } z = -h,\ 0 < x < B \tag{11}$$

Eq. (11) is the Darcy's model which indicates that the vertical mass fluxes between region 2 and 3 are continuous at the porous plate and the vertical flow velocity across the porous plate is linearly proportional to the pressure difference between each plate sides. The imaginary part of the proportionality constant σ is related to the inertia effect and thus has nothing to do with energy dissipation. It can be neglected when the porous plate is thin and the size of holes is not large. The positive real value of σ is called the porous-effect parameter and represents viscous effects and can directly be obtained from experiment. The porous-effect parameter G is recently defined as (see Cho and Kim (2013)):

$$G = \frac{2\pi\sigma}{k_0} \tag{12}$$

It is assumed that the plate deflection, slope of deflection, bending moment and shear force are continuous at x=0 and $x = B$, which yield

$$\left.\begin{aligned} &\phi_{jz} = \phi_{2z}, \quad \phi_{jxz} = \phi_{2xz}, \\ &EI\left(\partial_x^2 - \nu\mu_y^2\right)\phi_{jz} = EI\left(\partial_x^2 - \nu\mu_y^2\right)\phi_{2z}, \\ &\left[\left\{EI\partial_x^2 - (2-\nu)\mu_y^2\partial_x\right\} + T_c\partial_x\right]\phi_{jz} \\ &\quad = \left[\left\{EI\partial_x^2 - (2-\nu)\mu_y^2\partial_x\right\} + T_c\partial_x\right]\phi_{2z}, \end{aligned}\right\} \tag{13}$$

where j=1 at x=0 and j=4, at $x = B$. Finally, the radiation condition for oblique wave scattering by a floating elastic plate over porous bed yield

$$\phi_j(x, z) = \begin{cases} \left(I_0 e^{-i q_0 x} + R_0 e^{i q_0 x}\right)f_0(k_0, z), & j = 1, x \to -\infty \\ T_0 e^{-i q_0 x} f_0(k_0, z), & j = 4, x \to \infty \end{cases} \tag{14}$$

where I_0, R_0, and T_0 are the constants associated with the incident, reflected and transmitted wave amplitudes, respectively with $q_0 = \sqrt{k_0^2 - \mu_y^2}$ and $f_0(k_0, z)$ being the associated eigenfunctions.

3 Flexural-Gravity Waves in the Presence of an Infinitely Extended Submerged Porous Plate

In this section, it is assumed that both the floating elastic plate and submerged porous plate are infinitely extended in the horizontal direction as in Fig. 2. Further, one-dimensional plane progressive flexural-gravity wave is considered with the assumption that the deflection of the floating elastic plate is of the form $\eta = \mathrm{Re}\ \{\eta_0 e^{-i\ (p\ x - \omega\ t)}\}$ where η_0 is the amplitudes of the deflection of the floating plate. Thus, the velocity potential in this case is of the form

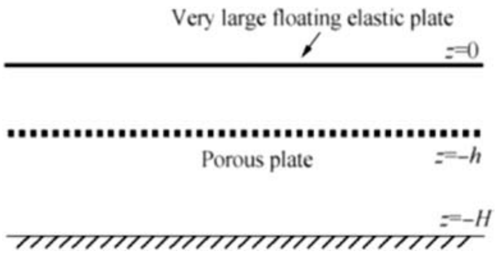

Fig. 2 Schematic diagram of flexural-gravity waves over a submerged infinitely extended porous plate

$$\Phi(x,z,t) = \begin{pmatrix} J_u(p,z) \\ J_l(p,z) \end{pmatrix} \eta \tag{15}$$

where

$$J_u(p,z) = \left(\frac{\mathrm{i}g}{\omega}\right) \frac{\cosh p(z+H) - F\sinh p(z+H)}{\cosh pH - F\sinh pH} \quad \text{for} -h < z < 0 \tag{16}$$

$$J_l(p,z) = \left(\frac{\mathrm{i}g}{\omega}\right) \frac{\tanh p(H-h) - F}{\tanh p(H-h)} \frac{\cosh p(z+H)}{\cosh pH - F\sinh pH} \quad \text{for} -H < z < -h \tag{17}$$

$$F = \frac{p\tanh^2 p(H-h)}{p\tanh p(H-h) - \mathrm{i}k_0 G\left\{1 - \tanh^2 p(H-h)\right\}} \tag{18}$$

with the wave number p satisfying the dispersion relation

$$\begin{aligned} K - \left(Dp^4 - Qp^2 + 1\right)p\tanh pH \\ = F\left\{K\tanh pH - p\left(Dp^4 - Qp^2 + 1\right)\right\} \end{aligned} \tag{19}$$

It may be noted that as $G \to \infty$, $F \to 0$, and the dispersion relation as in Eqs. (19) reduces to the dispersion relation associated with the floating elastic plate without submerged porous plate as in Karmakar et al. (2010) which in terms of k satisfies the relation

$$\left(Dk^4 - Qk^2 + 1\right)k\tanh kH = K. \tag{20}$$

In particular, for D=0, Q=0, and m_s=0, ($K = \omega^2/g$), the dispersion relations as in Eqs. (20) and (19) reduce to the dispersion relations for open water and submerged porous plate regions in case of gravity wave scattering by a submerged porous plate as in Liu et al. (2007). In the present study, the solution of the complex dispersion relation in Eq. (19) is the central to the solution method. The nature of the roots of the dispersion relation are obtained using the principle of counting argument as discussed in Fox and Squire (1990). In Fig. 3a, behavior of the roots of the dispersion as in Eqs. (20) is plotted. As earlier discussed by Fox and Squire (1990), it has two real roots k_0 and $-k_0$, four complex roots k_I, k_{II}, k_{III} and k_{IV} with $k_I = \overline{k}_{IV}$ and $k_{II} = \overline{k}_{III}$ and a sequence of purely imaginary roots $\pm k_n$, n=1, 2, 3,..., and are shown in the contour plot (as in Fig. 3a). However, all roots of the dispersion relation as in Eq. (19) are complex in nature (as in Fig. 3b) and which has certain close proximity with the roots discussed in Fig. 3a. The complex roots p_0 and $-p_0$ are referred as the wave numbers associated with the most progressive waves in flexural-gravity modes whilst, the four complex roots P_I, P_{II}, P_{III} and P_{IV} lying in the four quadrants are referred to wave numbers associated with the non-propagating wave modes. Further, the infinitely many complex roots p_j for j=2,3,.... which are close to the imaginary axis of the p-plane are referred as the evanescent wave modes. Assuming realistic nature of the physical

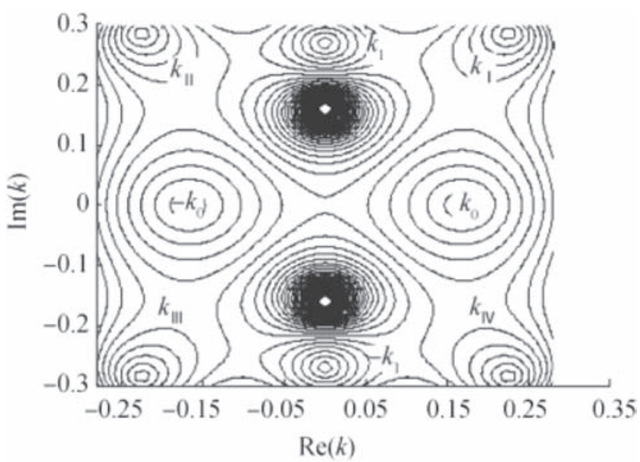

(a) Contour plot of Eq. (20)

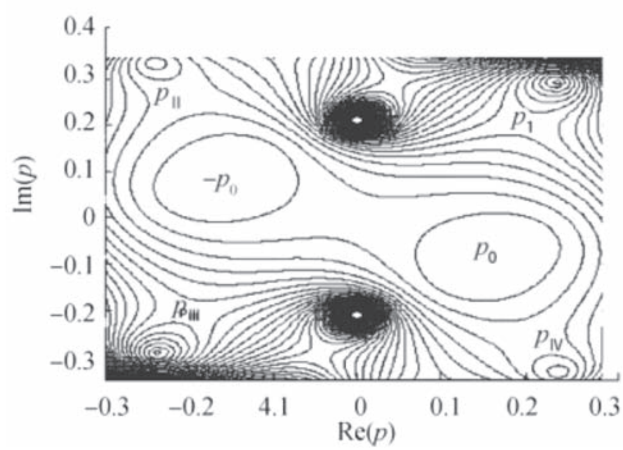

(b) Contour plot of Eq. (19)

Fig. 3 Contour plots of roots of the dispersion relation for **a** flexural-gravity wave without a porous plate and **b** flexural-gravity wave with a porous plate for H=10m, T=5s, g=9.81m/s^2, ν=0.3, G=1, E=5GPa, d=0.1 and T_c=0 problem, the velocity potentials are assumed to be bounded, and the roots of the dispersion relation in the first and fourth quadrants are used in the computation.

In Fig. 4a, b, phase velocities ω/p_0 versus real part of the positive wave number p_0 are plotted for different values of compressive forceT_c and depth ratio h/H, respectively. Figure 4a reveals that phase velocity in the absence of submerged porous plate ($G=\infty$) for T_c=2$(EI\rho g)^{1/2}$ is in close agreement with the result of Mohanty et al. (2014). Moroever, phase velocity decreases significantly in the presence of a solid submerged plate (G=0). In addition, phase velocity decreases with an increase in compressive force. On the other hand, Fig. 4b depicts that in the presence of an impermeable submerged plate (G=0), the phase velocity is less when the plate is close to the floating elastic plate. However, the critical value of the compressive force for which phase speed attains zero minimum is independent of the position of the submerged impermeable plate.

In Fig. 5a, b, c, the phase velocities versus submergence depth h/H are plotted for different values of porous-effect

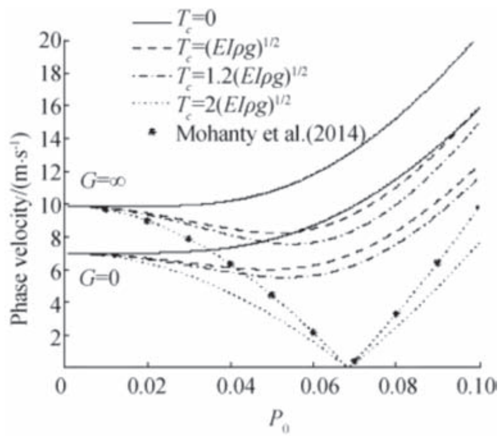

(a) Phase velocity

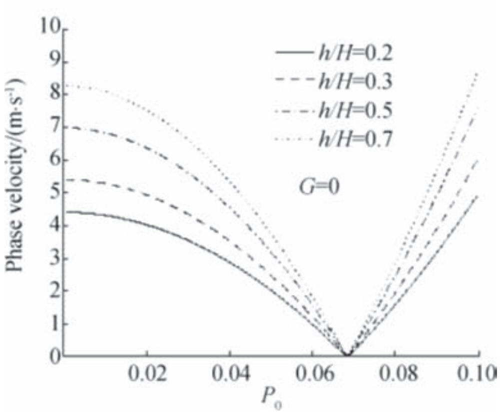

(b) Phase velocity

Fig. 4 Variation of phase velocity versus wave number p_0 for different values of **a** compressive force T_c and **b** depth ratio h/H with H=10 m, T=5s, ν=0.3, g=9.81 m/s^2 and E=5 GPa. In **a** h/H=0.5 and **b** T_c=2$(EI\rho g)^{1/2}$

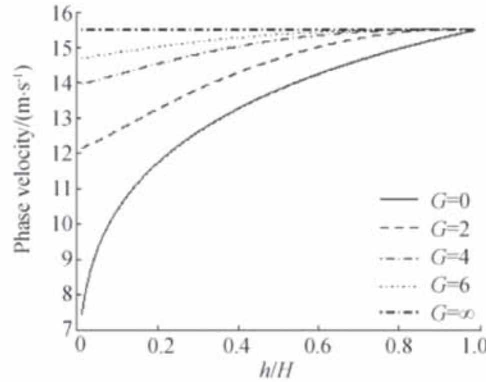

(a) Phase velocity

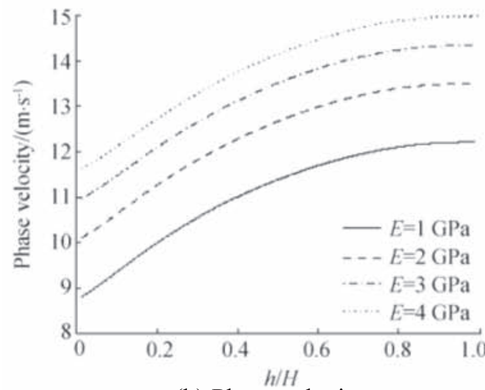

(b) Phase velocity

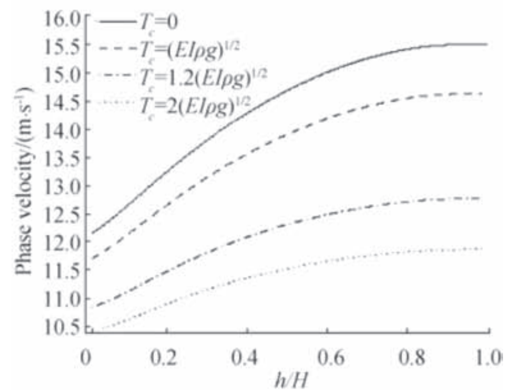

(c) Phase velocity

Fig. 5 Variation of phase velocity versus submergence depth h/H for different values of (a) porous-effect parameter G, (b) Young's modulus$E$and (c) compressive force T_c with H=10m, T=5s, ν=0.3, g=9.81m/s^2, d=1m. In (a) E=5GPa and T_c=0, (b) G=2 and T_c=0, (c) G=2 and E=5GPa

parameter G, Young's modulus E and compressive force T_c respectively. Figure 5a reveals that in the absence of submerged porous plate ($G=\infty$), the phase velocity is more compared to the presence of submerged porous plate. This is due to the dissipation of wave energy by the submerged porous plate.Further, the phase velocity is more when submergedplate is nearer to the floating plate. This is due to the fact that the wave energy concentration is more near the floating plate when the submerged plate is close to the floating plate.

In general, when the position of the submerged plate goes to the bottom, effect of submerged plate will be less on flexural-gravity wave motion. Thus, phase velocity increases with an increase in h/H. Moreover, the phase velocity increases with an increase in G. This is due to the fact that more wave transmit through the fine pores of the porous plate for higher values of G. In Fig. 5b, it is seen that rigidity of the floating plate has less effect on phase velocity when submerged plate is nearer to the floating plate. However, with an increase in Young's modulus E, the phase velocity increases for higher values of h/H. On the other hand, Fig. 5c reveals that phase velocity decreases with decrease in compressive force T_c.

In Fig. 6a, b, deflection of the floating plate η/H versus x/H is plotted for various values of porous-effect parameter G and submergence depth h/H respectively. Figure 6a reveals that in the absence of submerged plate ($G=\infty$), the amplitude of the floating plate is more and follows a periodic pattern. However, in the presence of the submerged plate, amplitude of floating plate decreases significantly and follows a decay pattern which is due the dissipation of wave energy by the porous structure. In addition, amplitude of the floating plate decreases rapidly and vanishes afterwards for lower value of porous-effect parameter G. From Fig. 6b, it is observed that the amplitude of the floating plate is less and decaying rate is more when submerged plate is becomes to nearer the floating plate. Thus, the submerged porous plate plays an important role in the reduction of the deflection of the floating elastic plate.

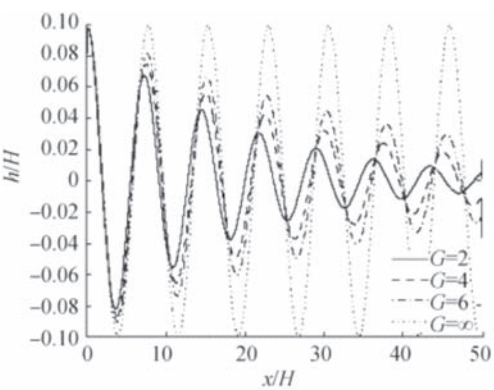

(a) Deflection

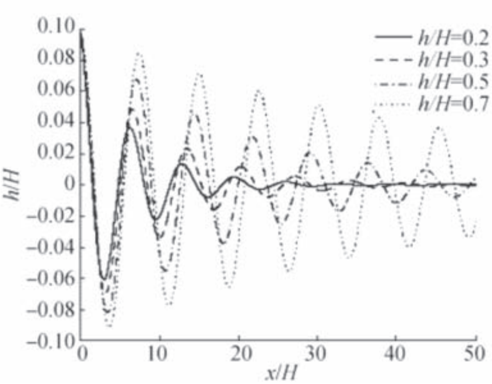

(b) Deflection

Fig. 6 Variation of deflection of the floating elastic plate versus x/H for different values of (a) porous-effect parameter G with h/H=0.5 and (b) submergence depth h/H with G=2 for H=10m, T=5s, ν=0.3, g=9.81m/s^2, d=1m, E=5GPa and T_c=0

4 Scattering of Flexural-Gravity Wave by a Finite Submerged Porous Plate

In this section, the solution procedure for oblique flexural-gravity wave being scattered by a finite submerged porous plate as in Fig. 1 is discussed briefly. All the boundary and matching conditions remain the same as discussed in Section 2. The spatial velocity potentials in regions 1, 2, 3 and 4 satisfying Eq. (7) along with boundary conditions in Eqs.(8) and (9) are written as

$$\phi_j = \begin{cases} I_0 e^{-i\, q_0\, x} f_{10}(k_0, z) + \sum\limits_{n=0}^{\infty} R_n e^{i\, q_n\, x} f_{1n}(k_n, z), x < 0,\ j = 1, \\ \sum\limits_{n=0}^{\infty} \left\{ A_n e^{-i\, Q_n\, x} + B_n e^{i\, Q_n (x-B)} \right\} f_{2n}(p_n, z),\ 0 < x < B,\ j = 2, \\ \sum\limits_{n=0}^{\infty} \left\{ A_n e^{-i\, Q_n\, x} + B_n e^{i\, Q_n\, (x-B)} \right\} f_{3n}(p_n, z),\ 0 < x < B,\ j = 3, \\ \sum\limits_{n=0}^{\infty} T_n e^{-i\, q_n\, (x-B)}\ f_{1n}(k_n, z), \qquad x > B,\ j = 4 \end{cases} \tag{21}$$

where A_n, B_n and T_n for n=0, I, II, 1, 2, … are the unknown coefficients to be determined with $q_n = \sqrt{k_n^2 - \mu_y^2}$ and $Q_n = \sqrt{p_n^2 - \mu_y^2}$. The eigenvalues k_n satisfy the dispersion relation as given in Eq. (20) for regions 1 and 4, and the eigenvalues p_n satisfy the dispersion relation for regions 2 and 3 is given in Eq. (19). Further, the eigenfunctions $f_{1n}(k_n, z)$, $f_{2n}(p_n, z)$ and $f_{3n}(p_n, z)$ are given by

$$f_{1n}(k_n, z) = \left(\frac{ig}{\omega}\right) \frac{\cosh k_n (z+H)}{\cosh k_n H}$$
$$f_{2n}(p_n, z) = J_l(p_n, z)$$
$$f_{3n}(p_n, z) = J_u(p_n, z)$$

The eigenfunction $f_{1n}(k_n, z)$ satisfy the orthogonal relation as given as

$$\langle f_{1m}, f_{1n} \rangle = \begin{cases} 0, & \text{for } m \neq n \\ E_n, & \text{for } m = n = 0, I, II, 1, 2, \ldots \end{cases} \tag{22}$$

with respect to the mode-coupling relation given by (as in Karmakar et al. (2010) and Mandal et al. (2017))

$$\left.\begin{aligned}\langle f_{1m}, f_{1n}\rangle = \int_{-H}^{0} f_{1m} f_{1n} \mathrm{d}z - \frac{Q}{K} f_{1m}'(0) f_{1n}'(0)\\ + \frac{D}{K}\left\{ f_{1m}''(0) f_{1n}'(0) + f_{1m}'(0) f_{1n}''(0)\right\}\end{aligned}\right\} \quad (23)$$

where

$$E_n = \frac{2\,k_n H\left(D\,k_n^4 - Q\,k_n^2 + 1\right) + \left(5D\,k_n^4 - 3Q\,k_n^2 + 1\right)\sinh 2\,k_n H}{4k_n\left(D\,k_n^4 - Q\,k_n^2 + 1\right)\cosh^2 k_n H} \quad (24)$$

Next, using mode-coupling relation (23) on the velocity potential $\phi_1(x, z)$ and eigenfunction $f_{1n}(z)$ along with the continuity of pressure as in Eq. (10) at x=0 yields

$$\begin{aligned}\langle \phi_1(0,z), f_{1m}(z)\rangle &= \int_{-H}^{0} \phi_1(0,z) f_{1m}(z)\mathrm{d}z - \frac{Q}{K}\phi_{1z}(0,0) f_{1m}'(0)\\ &+ \frac{D}{K}\left\{\phi_{1zzz}(0,0) f_{1m}'(0) + \phi_{1z}(0,0) f_{1m}''(0)\right\}\\ &= \int_{-H}^{-h} \phi_3(0,z) f_{1m}(z)\mathrm{d}z + \int_{-h}^{0}\phi_2(0,z) f_{1m}(z)\mathrm{d}z\\ &- \frac{Q}{K}\beta_{10} f_{1m}'(0) + \frac{D}{K}\left\{\beta_{30} f_{1m}'(0) + \beta_{10} f_{1m}''(0)\right\}\end{aligned} \quad (25)$$

where $\beta_{10} = \phi_{1z}(0, 0)$ and $\beta_{30} = \phi_{1zzz}(0, 0)$ for m=0, I, II, 1, 2, …. Further, using the orthogonal property of the eigenfunction $f_{1m}(z)$ as in Eq. (22) and the velocity potentials as in Eq. (21) yields

$$\left.\begin{aligned}R_m\langle f_{1m}(z), f_{1m}(z)\rangle - \sum_{n=0}^{\infty}\left(A_n + B_n \mathrm{e}^{-\mathrm{i}Q_n b}\right)\left(Y_{nm} + Z_{nm}\right)\\ -\beta_{10}\left\{\frac{D}{K} f_{1m}''(0) - \frac{Q}{K} f_{1m}''(0) f_{1m}'(0)\right\}\\ -\beta_{30}\left\{\frac{D}{K} f_{1m}'(0)\right\} = I_0\delta_m,\end{aligned}\right\} \quad (26)$$

where

$$\delta_m = \begin{cases} 0, & \text{for } m = I, II, 1, 2..., \\ \langle f_{1m}, f_{1n}\rangle, & \text{for } m = 0\end{cases} \quad Y_{nm} = \int_{-h}^{0} f_{2n}(z), f_{1m}(z)\mathrm{d}z,\ Z_{nm} = \int_{-H}^{-h} f_{3n}(z), f_{1m}(z)\mathrm{d}z$$

Similarly, using continuity of velocity as in Eq. (10) and mode-coupling relation (23) on the velocity potential $\phi_1(x, z)$ and eigenfunction $f_{1n}(z)$ at x=0 yields

$$\left.\begin{aligned}\langle \phi_{1x}(0,z), f_{1m}(z)\rangle &= \int_{-H}^{0} \phi_{1x}(0,z) f_{1m}(z)\mathrm{d}z - \frac{Q}{K}\phi_{1xz}(0,0) f_{1m}'(0)\\ &+ \frac{D}{K}\left\{\phi_{1xzzz}(0,0) f_{1m}'(0) + \phi_{1xz}(0,0) f_{1m}''(0)\right\}\\ &= \int_{-H}^{-h} \phi_{3x}(0,z) f_{1m}(z)\mathrm{d}z + \int_{-h}^{0}\phi_{2x}(0,z) f_{1m}(z)\mathrm{d}z\\ &- \frac{Q}{K}\beta_{20} f_{1m}'(0) + \frac{D}{K}\left\{\beta_{40} f_{1m}'(0) + \beta_{20} f_{1m}''(0)\right\}\end{aligned}\right\} \quad (27)$$

where $\beta_{20} = \phi_{1xz}(0, 0)$ and $\beta_{40} = \phi_{1xzzz}(0, 0)$ for m=0, I, II, 1, 2, …. Further, using the orthogonal property of the eigenfunction $f_{1m}(z)$ as in Eq. (22) and the velocity potentials as in Eq. (21) yields

$$\left.\begin{aligned}\mathrm{i}q_m R_m\langle f_{1m}(z), f_{1m}(z)\rangle - \sum_{n=0}^{\infty}\left(-A_n + B_n\mathrm{e}^{-\mathrm{i}Q_n b}\right)\mathrm{i}Q_n\left(Y_{nm} + Z_{nm}\right)\\ -\beta_{20}\left\{\frac{D}{K} f_{1m}''(0) - \frac{Q}{K} f_{1m}''(0) f_{1m}'(0)\right\} - \beta_{40}\left\{\frac{D}{K} f_{1m}'(0)\right\} = \mathrm{i}I_0 q_0 \delta_m\end{aligned}\right\} \quad (28)$$

Moreover, using mode-coupling relation (23) on the velocity potential $\phi_4(x, z)$ and eigenfunction $f_{1n}(z)$ along with the continuity of pressure as in Eq. (10) at $x = B$ yields

$$\begin{aligned}\langle \phi_4(B,z), f_{1m}(z)\rangle &= \int_{-H}^{0} \phi_4(B,z) f_{1m}(z)\mathrm{d}z - \frac{Q}{K}\phi_{4z}(B,0) f_{1m}'(0)\\ &+ \frac{D}{K}\left\{\phi_{4zzz}(B,0) f_{1m}'(0) + \phi_{4z}(B,0) f_{1m}''(0)\right\}\\ &= \int_{-H}^{-h} \phi_3(B,z) f_{1m}(z)\mathrm{d}z + \int_{-h}^{0}\phi_2(B,z) f_{1m}(z)\mathrm{d}z\\ &- \frac{Q}{K}\beta_{1b} f_{1m}'(0) + \frac{D}{K}\left\{\beta_{3b} f_{1m}'(0) + \beta_{1b} f_{1m}''(0)\right\}\end{aligned} \quad (29)$$

where $\beta_{1b} = \phi_{4z}(B, 0)$ and $\beta_{3b} = \phi_{4zzz}(B, 0)$ for m=0, I, II, 1, 2, …. Further, using the orthogonal property of the eigenfunction $f_{1m}(z)$ as in Eq. (22) and the velocity potentials as in Eq. (21) yields

$$\begin{aligned}T_m\langle f_{1m}(z), f_{1m}(z)\rangle - \sum_{n=0}^{\infty}\left(A_n\mathrm{e}^{-\mathrm{i}Q_n b} + B_n\right)\left(Y_{nm} + Z_{nm}\right)\\ -\beta_{1b}\left\{\frac{D}{K} f_{1m}''(0) - \frac{Q}{K} f_{1m}''(0) f_{1m}'(0)\right\} - \beta_{3b}\left\{\frac{D}{K} f_{1m}'(0)\right\} = 0\end{aligned} \quad (30)$$

In addition, using continuity of velocity as in Eq. (10) and mode-coupling relation (23) on the velocity potential $\phi_4(x, z)$ and eigenfunction $f_{1n}(z)$ at $x = B$ yields

$$\begin{aligned}&\langle \phi_{4x}(B,z), f_{1m}(z)\rangle = \int_{-H}^{0}\phi_{4x}(B,z)f_{1m}(z)\mathrm{d}z \\ &-\frac{Q}{K}\phi_{4xz}(B,0)f_{1m}{'}(0) + \frac{D}{K}\left\{\phi_{4xzzz}(B,0)f_{1m}{'}(0) + \phi_{4xz}(B,0)f_{1m}{'''}(0)\right\} \\ &= \int_{-H}^{-h}\phi_{3x}(B,z)f_{1m}(z)\mathrm{d}z + \int_{-h}^{0}\phi_{2x}(B,z)f_{1m}(z)\mathrm{d}z \\ &-\frac{Q}{K}\beta_{2b}f_{1m}{'}(0) + \frac{D}{K}\left\{\beta_{4b}f_{1m}{'}(0) + \beta_{2b}f_{1m}{'''}(0)\right\}\end{aligned} \tag{31}$$

where $\beta_{2b} = \phi_{4xz}(B, 0)$ and $\beta_{4b} = \phi_{4xzzz}(B, 0)$ for m=0, I, II, 1, 2, …. Using the orthogonal property of the eigenfunction $f_{1m}(z)$ as in Eq. (22) and the velocity potentials as in Eq. (21) yields

$$\begin{aligned}&\mathrm{i}q_m T_m\langle f_{1m}(z), f_{1m}(z)\rangle - \sum_{n=0}^{\infty}\left(A_n\mathrm{e}^{-\mathrm{i}Q_n b} + B_n\right)\mathrm{i}Q_n\left(Y_{nm} + Z_{nm}\right) \\ &-\beta_{2b}\left\{\frac{D}{K}f_{1m}{'''}(0) - \frac{Q}{K}f_{1m}{'''}(0)f_{1m}{'}(0)\right\} - \beta_{4b}\left\{\frac{D}{K}f_{1m}{'}(0)\right\} = 0\end{aligned} \tag{32}$$

Truncating the infinite series up to N terms, from (26), (28), (30), and (32), it can be found a linear system of 4N equations. Utilizing the continuity conditions as in Eq. (13) for the plate deflection, slope of deflection, bending moment and shear forces at (0,0), which yield

$$\sum_{n=0}^{N} R_n k_n \tanh(k_n H) - \beta_{10} = I_0 k_0 \tanh(k_0 H) \tag{33}$$

$$\sum_{n=0}^{N} R_n q_n k_n \tanh(k_n H) + \mathrm{i}\beta_{20} = I_0 q_0 k_0 \tanh(k_0 H) \tag{34}$$

$$\begin{aligned}&\sum_{n=0}^{N} R_n\left(q_n^2 + \nu\mu_y^2\right)k_n\tanh(k_n H) + \frac{\beta_{30}}{EI} \\ &\quad = -I_0\left(q_0^2 + \nu\mu_y^2\right)k_0\tanh(k_0 H)\end{aligned} \tag{35}$$

$$\begin{aligned}&\sum_{n=0}^{N} R_n q_n k_n \tanh(k_n H)\left[EI\left\{q_n^2 + \left((2-\nu)\mu_y^2\right\} - Q\right] - \mathrm{i}\beta_{40} \\ &\qquad = I_0 q_0 k_0 \tanh(k_0 H)\left[EI\left\{q_0^2 + (2-\nu)\mu_y^2\right\} - Q\right]\end{aligned} \tag{36}$$

Similarly, utilizing the continuity conditions as in Eq. (13) for the plate deflection, slope of deflection, bending moment, and shear forces at $(B, 0)$, which yield

$$\sum_{n=0}^{N} T_n k_n \tanh(k_n H) + \beta_{1b} = 0 \tag{37}$$

$$\sum_{n=0}^{N} T_n q_n k_n \tanh(k_n H) - \mathrm{i}\beta_{2b} = 0 \tag{38}$$

$$\sum_{n=0}^{N} T_n\left(q_n^2 + \nu\mu_y^2\right)k_n\tanh(k_n H) - \frac{\beta_{3b}}{EI} = 0 \tag{39}$$

$$\sum_{n=0}^{N} T_n q_n k_n \tanh(k_n H)\left[EI\left\{q_n^2 + (2-\nu)\mu_y^2\right\} - Q\right] + \mathrm{i}\beta_{4b} = 0 \tag{40}$$

Finally, using Eqs. (33)–(40), a linear system of (4N +8) equations is obtained for the determination of unknowns as given by R_0, R_I, R_{II}, $R_1,\ldots,R_n, A_0, A_I, A_{II}, A_1,\ldots,A_n, B_0, B_I, B_{II}, B_1,\ldots,B_n, T_0, T_I, T_{II}, T_1,\ldots,T_n, \beta_{10}$, $\beta_{20}, \beta_{30}, \beta_{40}, \beta_{1b}, \beta_{2b}, \beta_{3b}$, and β_{4b} . The determination of the unknowns will in turn provide the velocity potentials in the respective regions. To analyze the effects of the submerged plate on flexural-gravity wave motion, various wave and structural parameters on the reflection, transmission and dissipation coefficients are computed and analyzed. Unless stated otherwise, physical parameters such as h/H=0.5, T=5s, B/H=1, G=2, g=9.81m/s^2, θ=30º, ν=0.3, E=1GPa, d=0.1m, and T_c=0 are kept fixed. From the general solution, physical quantities such as reflection, transmission, and dissipation coefficients, K_r, K_t, and K_d respectively are computed using the formulae

$$K_r = \left|\frac{R_0}{I_0}\right|, \quad K_t = \left|\frac{T_0}{I_0}\right| \tag{41}$$

and

$$K_d = 1 - \left(K_r^2 + K_t^2\right) \tag{42}$$

In Table 1, numerical values of reflection, transmission and dissipation coefficients are computed for different values of N for certain fixed values of k_0H. Here, N=0 represents the

Table 1 Convergence of the reflection and transmission coefficients for different values of N and nondimensional wave number K_0H for $E = 1$ GPa, $T_c = 0$, $B/H = 1$, $h/H = 0.5$, $G = 2$ an d $\theta = 0^\circ$

	k_0H=0.5		k_0H=1		k_0H=2		k_0H=3		k_0H=4	
N	K_r	K_t	K_r	K_t	K_r	K_t	K_r	K_t	K_r	K_t
0	0.1012	0.9104	0.2415	0.7895	0.3993	0.5607	0.4389	0.3700	0.4501	0.1968
3	0.1960	0.8939	0.4320	0.7113	0.6947	0.3557	0.7043	0.1735	0.2589	0.1696
5	0.1959	0.8938	0.4311	0.7117	0.6910	0.3571	0.6972	0.1743	0.2450	0.1634
10	0.1958	0.8938	0.4308	0.7118	0.6903	0.3577	0.6968	0.1749	0.2442	0.1635
15	0.1958	0.8938	0.4308	0.7118	0.6903	0.3577	0.6968	0.1749	0.2442	0.1635

progressive flexural-wave mode solution. Table 1 demonstrates that the numerical results converge up to 4 decimal accuracy for N larger than 15.

In the absence of floating elastic plate, to validate the present computation with the standard results available in the literature, in Fig. 7a, the reflection and transmission coefficients are plotted as a function of wave number K_0H with $D = 0$, $Q = 0$ and $m_s = 0$. Figure 7a reveals that the results agree well with that of Fig. 3 of Cho and Kim (2013) for surface gravity wave scattering by a submerged porous plate. On the other hand, in Fig. 7b, c, d, the reflection, transmission, and dissipation coefficients versus non-dimensional wave number K_0H are plotted respectively, in the presence of floating elastic plate for different values of porous-effect parameter G. Fig. 7a, b reveals that in case of solid plate ($G = 0$), there exist high wave reflection and low transmission. In this case also, full reflection and zero transmission can be found for higher values of flexural-gravity wave number K_0H. However, full reflection and zero transmission do not occur in the presence of the submerged porous plate. Further, wave reflection decreases, wave transmission increases, and dissipation coefficient decreases with an increase in porous-effect parameter G due to loss of wave energy by the porous plate. In addition, in case of porous

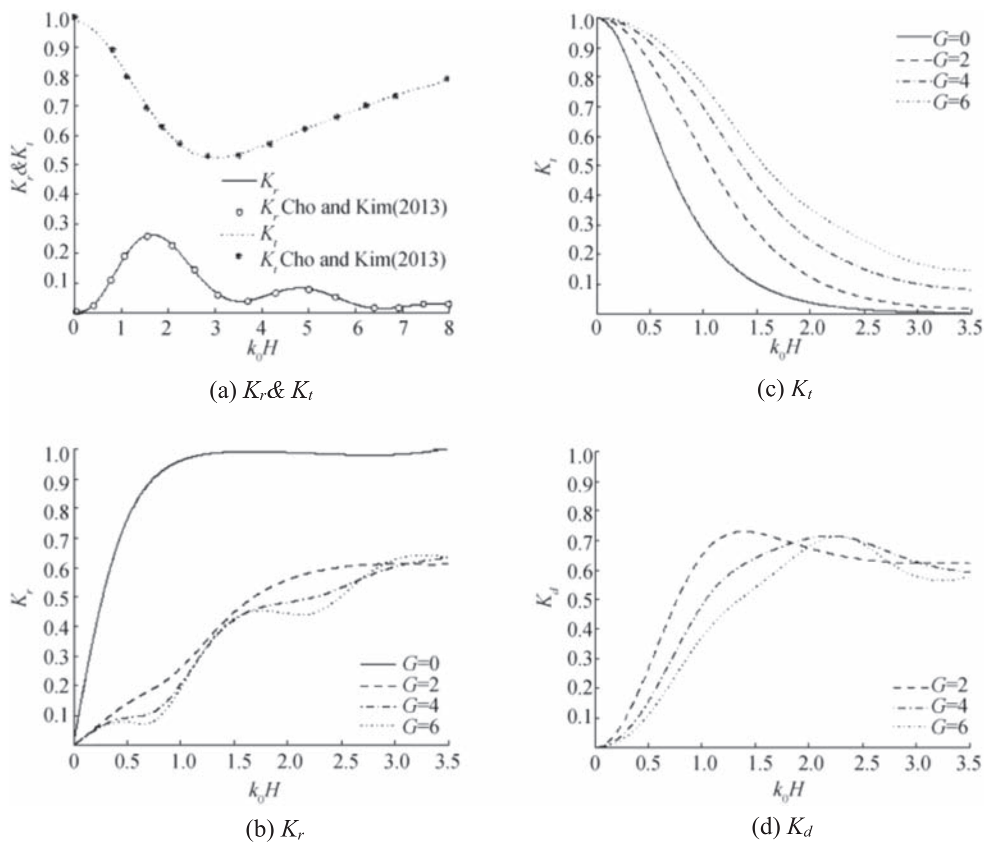

Fig. 7 Variation of the **a** K_r and K_t versus K_0H in the absence of floating elastic plate with $B/H = 1$, $\theta = 30^\circ$ and $h/H = 0.5$, and **b** K_r, **c** K_t, and **d** K_d versus in the presence floating elastic plate for different values K_0H of porous-effect parameter G with $h/H = 0.5$, $B/H = 1$, $\theta = 30^\circ$, $E = 1$GPa and $T_c = 0$

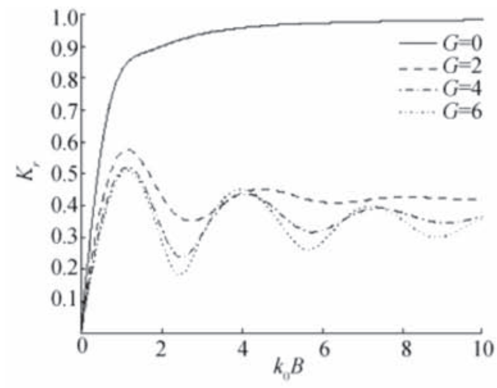

(a) K_r

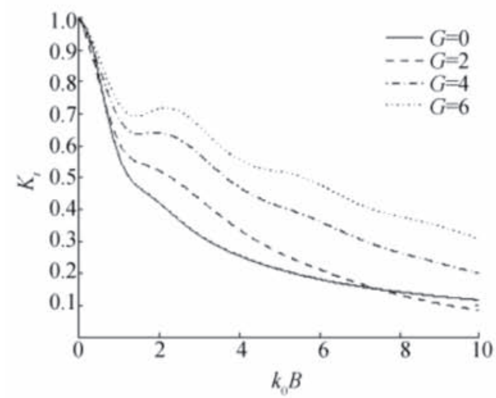

(b) K_t

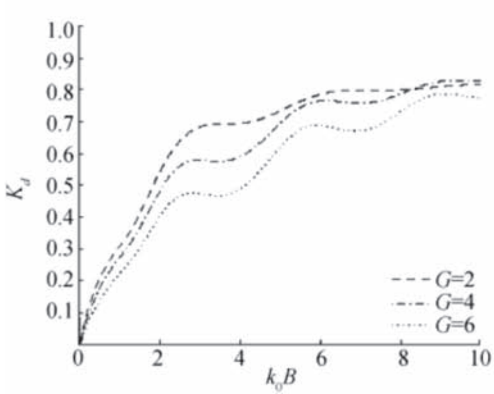

(c) K_d

Fig. 8 Variation of the **a** reflection coefficient K_r, **b** transmission coefficient K_t, and **c** dissipation coefficient K_d versus non-dimensional length of the porous plate K_0B for different values of porous-effect parameter G with $h/H = 0.5$, $\theta = 30^\circ$, $E = 1$GPa and $T_c = 0$

plate, with an increase in G, the reflection and dissipation coefficients follows certain oscillatory pattern, while wave transmission becomes negligible. In thepresence of the submerged plate, a part of the wave energy loss takes place due to the interference of the incident and reflected

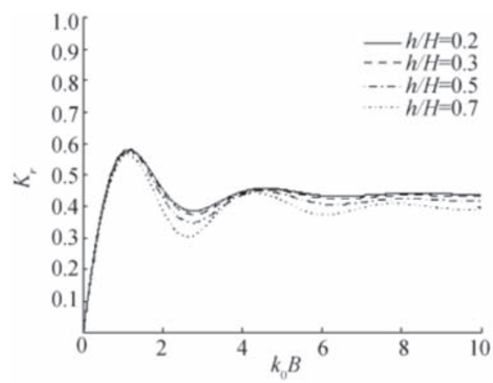

(a) K_r

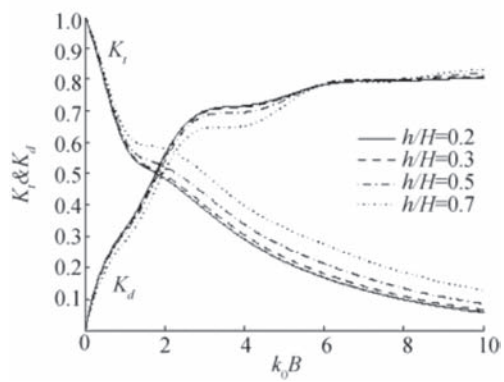

(b) K_t & K_d

Fig. 9 Variation of the **a** reflection coefficient K_r, and **b** transmission and dissipation coefficients $K_t$and K_d versus non-dimensional length of the porous plate K_0B for different values of submergence depth h/H with $G = 2$, $\theta = 30^\circ$, $E = 1$GPa and $T_c = 0$

waves, while another part of energy is dissipated while passing through the porous structure. Thus, a very small portion of the incident wave energy transmit after passing through the porous structure.

In Fig. 8a, b, c, the reflection, transmission, and dissipation coefficients versus non-dimensional length of the porous plate K_0B are plotted respectively, for different values of porous effect parameter G. Figure 8a depicts that with an increase in K_0B, initially the reflection coefficient increases and then decreases uniformly for larger values of K_0b. On the other hand, Fig. 8b, c reveals that the transmission coefficient K_t decreases and dissipation coefficient K_d increases with increase in the absolute value of the porous-effect parameter G and structural length. However, for impermeable plate with $G = 0$, no energy loss takes place. Moreover, energy loss is more for higher values of non-dimensional plate length K_0B as larger amount of energy dissipation takes place for larger plate. Further, as the plate length approaches zero, all wave energy will transmit and there is no loss takes place as expected.

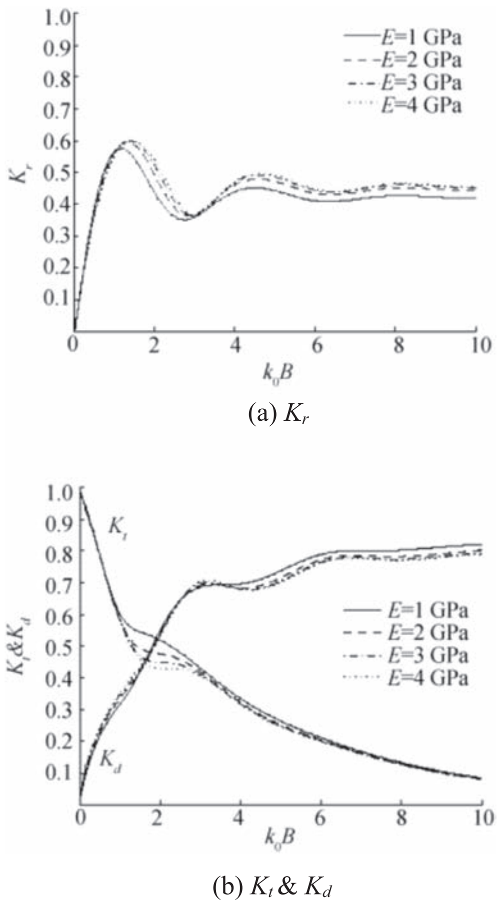

Fig. 10 Variation of the **a** reflection coefficient K_r, and **b** transmission and dissipation coefficients K_t and K_d versus non-dimensional length of the porous plate K_0B for different values of Young's modulus E with $G = 2$, $\theta = 30^\circ$, $E = 1$GPa and $T_c = 0$

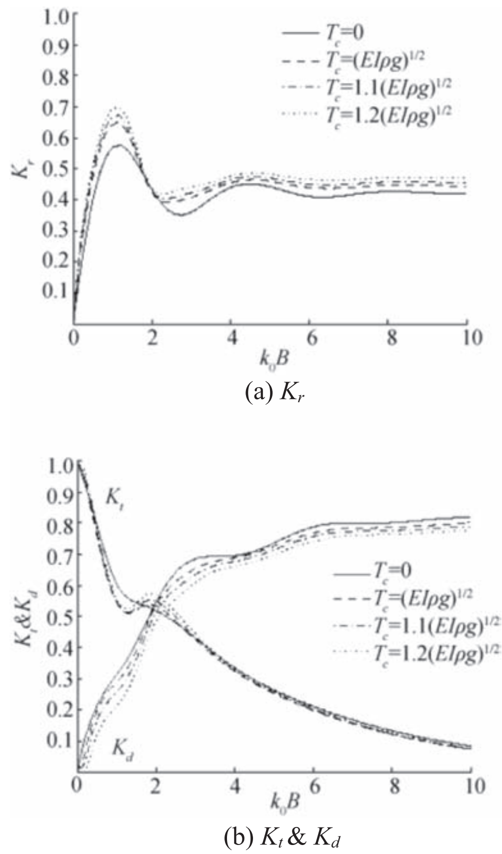

Fig. 11 Variation of the (a) Reflection coefficient K_r, and (b) transmission and dissipation coefficients K_t and K_d versus non-dimensional length of the porous plate K_0B for different values of the compressive force $T_c$with $G = 2$, $\theta = 30^\circ$, $h/H = 0.5$ and $E = 1$GPa

In Fig. 9a, b, the reflection, transmission, and dissipation coefficients versus non-dimensional length of the porous plate K_0B are plotted respectively, for different values of submergence depth h/H.The general pattern in wave reflection, transmission and dissipation coefficients are similar to the observation in Fig. 8. It is seen that the reflection and dissipation coefficients increase, and transmission coefficient decreases as the submerged plate becomes nearer to the floating plate. This is due to the fact that when the submerged plate is near to the surface, a major portion of the wave energy which concentrates near the floating plate is reflected by the plate and another part is dissipated by the horizontal submerged porous plate.

Further, certain shift in the optimum values in the reflection coefficient is observed which is due to the constructive/destructive interference of the incident and reflected waves. However, significant decrease in the oscillatory pattern in transmission coefficient is observed with an increase in K_0B due to the dissipation of wave energy while passing through the submerged flexible porous plate.

In Fig. 10a, b, the reflection, transmission and dissipation coefficients versus nondimensional length of the porous plate K_0B are plotted, respectively, for different values of Young's modulus E of the plate. From these figures, it is found that the wave reflection increases with an increase in Young's modulus E of the floating elastic plate. However, wave transmission decreases with an increase in E.

In Fig. 11a, b, the reflection, transmission, and dissipation coefficients versus the non-dimensional length of the porous plate K_0B are plotted respectively, for different values of compressive force T_c. From Fig. 11a, it is observed that the reflection coefficient increases and dissipation coefficient decreases with an increase incompressive force. However, there is a negligible effect in wave transmission with an increase in T_c.

In Fig. 12a, b, the reflection and transmission coefficients versus angle of incidence θ are plotted respectively, for different values of porous-effect parameter G. From these figures, it is found that the wave reflection increases with an increase in angle of incidence θ, while an opposite trend is observed for wave transmission. Further, the wave reflection decreases with an increase in the porous-effect parameter G, while an opposite trend is observed for wave transmission.

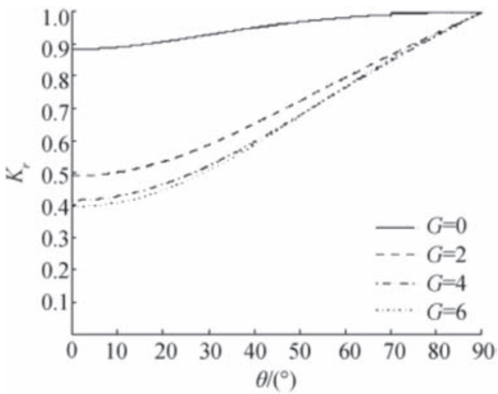

(a) K_r

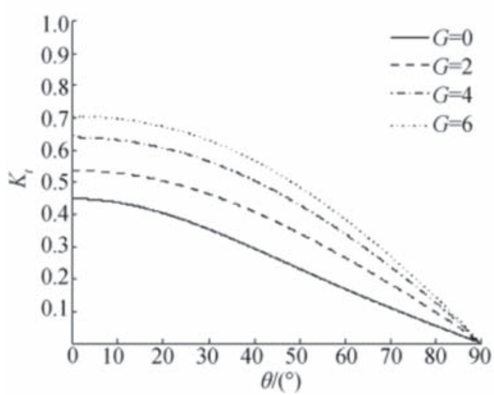

(b) K_t

Fig. 12 Variation of the **a** reflection coefficient K_r and **b** transmission coefficient K_t versus angle of incidence θ for different values of the porous-effect parameter G with $h/H = 0.5$, $T_c = 0$ and $E = 1$GPa

5 Conclusion

In the present study, a model is developed to study scattering of oblique flexural-gravity waves by submerged horizontal porous plate. The problem is solved by means of eigenfunction expansions method and the associated orthogonal mode-coupling relations. Our results reveal that the phase velocity and the amplitude of the deflection of the floating elastic plate will significantly decrease in the presence of a submerged porous plate. In particular, plate deflection will follow a kind of decaying pattern in the presence of submerged porous plate. Moreover, the study reveals that the presence of a finite horizontal submerged plate will often lead to full energy reflection and zero transmission which is due to the constructive interference of the incident and reflected waves. Also, with the introduction of structural porosity, incident wave can be partially reflected even if wave transmission is zero, a consequence of dissipation of wave energy by the porous structure. Wave transmission may decrease significantly with an increase in the length of the submerged plate, while the porous-effect parameter plays an important role in the wave energy dissipation. In addition, wave reflection increases while wave transmission decreases as the submerged plate becomes closer to the floating plate. Thus, with the help of a submerged porous plate of finite length, the structural response of the floating structure can be reduced significantly, which will be of immense importance in the design of a very large floating structure. Since energy transmitted onto the lee side of the submerged structure is negligible, wave-induced structural vibration of a large floating structure can also be much reduced with the aid of a submerged porous structure.

References

Behera H, Ng CO (2017) Oblique wave scattering by a system of floating and submerged porous elastic plates. In: Proceedings of the 32nd International Workshop on Water Waves and Floating Bodies (IWWWFB32), Dalian, China, April 23–26

Behera H, Sahoo T (2015) Hydroelastic analysis of gravity wave interaction with submerged horizontal flexible porous plate. J Fluids Struct 54:643–660. https://doi.org/10.1016/j.jfluidstructs.2015.01.005

Chakrabarti A, Ahluwalia D, Manam S (2003) Surface water waves involving a vertical barrier in the presence of an ice-cover. Int J Eng Sci 41:1145–1162. https://doi.org/10.1016/S0020-7225(02)00375-0

Cheng Y, Zhai G, Ou J (2015) Numerical and experimental analysis of hydroelastic response on a very large floating structure edged with a pair of submerged horizontal plates. J Mar Sci Technol 20:127–141. https://doi.org/10.1007/s00773-014-0269-y

Cheng Y, Ji C, Zhai G, Oleg G (2016) Dual inclined perforated anti-motion plates for mitigating hydroelastic response of a VLFS under wave action. Ocean Eng 121:572–591. https://doi.org/10.1016/j.oceaneng.2016.05.044

Cho I, Kim M (1998) Interactions of a horizontal flexible membrane with oblique incident waves. J Fluid Mech 367:139–161. https://doi.org/10.1017/S0022112098001499

Cho I, Kim M (2000) Interactions of horizontal porous flexible membrane with waves. J Waterw Port Coast Ocean Eng 126:245–253. https://doi.org/10.1061/(ASCE)0733-950X(2000)126:5(245)

Cho I, Kim M (2013) Transmission of oblique incident waves by a submerged horizontal porous plate. Ocean Eng 61:56–65. https://doi.org/10.1016/j.oceaneng.2012.12.044

Das D, Mandal B (2009) Wave scattering by a circular cylinder half-immersed in water with an ice-cover. Int J Eng Sci 47:463–474. https://doi.org/10.1016/j.ijengsci.2008.10.001

Das S, Sahoo T (2017) Hydroelastic analysis of very large floating structure over viscoelastic bed. Meccanica 52:1871–1887. https://doi.org/10.1007/s11012-016-0529-5

Das S, Behera H, Sahoo T (2016) Flexural gravity wave motion over poroelastic bed. Wave Motion 63:135–148. https://doi.org/10.1016/j.wavemoti.2016.02.002

Evans DV, Peter MA (2011) Asymptotic reflection of linear water waves by submerged horizontal porous plates. J Eng Math 69:135–154. https://doi.org/10.1007/s10665-009-9355-2

Fox C, Squire VA (1990) Reflection and transmission characteristics at the edge of shore fast sea ice. J Geophys Res Oceans 95:11629–11639. https://doi.org/10.1029/JC095iC07p11629

Fu S, Moan T, Chen X, Cui W (2007) Hydroelastic analysis of flexible floating interconnected structures. Ocean Eng 34:1516–1531. https://doi.org/10.1016/j.oceaneng.2007.01.003

Hassan ULM, Meylan MH, Peter M (2009) Water-wave scattering by submerged elastic plates. Q J Mech Appl Math 62:321–344. https://doi.org/10.1093/qjmam/hbp008

Heins AE (1950) Water waves over a channel of finite depth with a submerged plane barrier. Can J Math 2:210–222. https://doi.org/10.4153/CJM-1950-019-2

Hu HH, Wang KH (2005) Damping effect on waves propagating past a submerged horizontal plate and a vertical porous wall. J Eng Mech 131:427–437. https://doi.org/10.1061/(ASCE)0733-9399(2005)131:4(427)

Ijima T, Ozaki S, Eguchi Y, Kobayashi A (1970) Breakwater and quay well by horizontal plates. Coast Eng 1970:1537–1556. https://doi.org/10.1061/9780872620285.094

Karmakar D, Bhattacharjee J, Sahoo T (2010) Oblique flexural gravity-wave scattering due to changes in bottom topography. J Eng Math 66:325–341. https://doi.org/10.1007/s10665-009-9297-8

Koley S, Sahoo T (2017) Oblique wave scattering by horizontal floating flexible porous membrane. Meccanica 52:125–138. https://doi.org/10.1007/s11012-016-0407-1

Liu Y, Li YC (2011) An alternative analytical solution for water-wave motion over a submerged horizontal porous plate. J Eng Math 69:385–400. https://doi.org/10.1007/s10665-010-9406-8

Liu Y, Li YC, Teng B (2007) Wave interaction with a perforated wall breakwater with a submerged horizontal porous plate. Ocean Eng 34:2364–2373. https://doi.org/10.1016/j.oceaneng.2007.05.002

Maiti P, Mandal B (2010) Wave scattering by a thin vertical barrier submerged beneath an ice-cover in deep water. Appl Ocean Res 32:367–373. https://doi.org/10.1016/j.apor.2010.07.001

Manam S, Kaligatla R (2011) Effect of a submerged vertical barrier on flexural gravity waves. Int J Eng Sci 49:755–767. https://doi.org/10.1016/j.ijengsci.2011.03.015

Mandal S, Sahoo T, Chakrabarti A (2017) Characteristics of eigen-systems for flexural gravity wave problems. Geophys Astrophys Fluid Dyn 111:249–281. https://doi.org/10.1080/03091929.2017.1318129

Meylan MH, Bennetts LG, Peter MA (2017) Water-wave scattering and energy dissipation by a floating porous elastic plate in three dimensions. Wave Motion 70:240–250. https://doi.org/10.1016/j.wavemoti.2016.06.014

Mohanty S, Mondal R, Sahoo T (2014) Time dependent flexural gravity waves in the presence of current. J Fluids Struct 45:28–49. https://doi.org/10.1016/j.jfluidstructs.2013.11.018

Mohapatra S, Sahoo T (2014a) Wave interaction with a floating and submerged elastic plate system. J Eng Math 87:47–71. https://doi.org/10.1007/s10665-013-9659-0

Mohapatra S, Sahoo T (2014b) Oblique wave diffraction by a flexible floating structure in the presence of a submerged flexible structure. Geophys Astrophys Fluid Dyn 108:615–638. https://doi.org/10.1080/03091929.2014.937806

Mondal R, Sahoo T (2012) Wave structure interaction problems for two-layer fluids in three dimensions. Wave Motion 49:501–524. https://doi.org/10.1016/j.wavemoti.2012.02.002

Mondal R, Sahoo T (2014) Wave structure interaction problems in three-layer fluid. Z Angew Math Phys 65:349–375. https://doi.org/10.1007/s00033-013-0368-3

Mondal R, Mohanty S, Sahoo T (2013) Expansion formulae for wave structure interaction problems in three dimensions. IMA J Appl Math 78:181–205. https://doi.org/10.1093/imamat/hxr044

Ohta H, Torii T, Hayashi N, Watanabe E, Utsunomiya T, Sekita K, Sunahara S (1999) Effect of attachment of a horizontal/vertical plate on the wave response of a VLFS. Proceedings of the third International Workshop on Very Large Floating Structure, University of Hawaii at Manao Honolulu, HI. pp 256–274

Squire VA (2011) Past, present and impendent hydroelastic challenges in the polar and subpolar seas. Philos Trans R Soc Lond A 369:2813–2831. https://doi.org/10.1098/rsta.2011.0093

Takagi K, Shimada K, Ikebuchi T (2000) An anti-motion device for a very large floating structure. Mar Struct 13:421–436. https://doi.org/10.1016/S0951-8339(00)00018-6

Tavana H, Khanjani M (2013) Reducing hydroelastic response of very large floating structure: a literature review. Int J Comput Appl 71:13–17. https://doi.org/10.5120/12353-8658

Wang C, Tay Z (2011) Very large floating structures: applications, research and development. Procedia Eng 14:62–72. https://doi.org/10.1016/j.proeng.2011.07.007

Wang C, Tay Z, Takagi K, Utsunomiya T (2010) Literature review of methods for mitigating hydroelastic response of VLFS under wave action. Appl Mech Rev 63:030802. https://doi.org/10.1115/1.4001690

Watanabe E, Utsunomiya T, Kuramoto M, Ohta H, Torii T, Hayashi N et al (2003) Wave response analysis of VLFS with an attached submerged plate. Int J Offshore Polar Eng 13

Williams T, Meylan MH (2012) The Wiener–Hopf and residue calculus solutions for a submerged semi-infinite elastic plate. J Eng Math 75:81–106. https://doi.org/10.1007/s10665-011-9518-9

Yoon JS, Cho SP, Jiwinangun RG, Lee PS (2014) Hydroelastic analysis of floating plates with multiple hinge connections in regular waves. Mar Struct 36:65–87. https://doi.org/10.1016/j.marstruc.2014.02.002

Yu X (2002) Functional performance of a submerged and essentially horizontal plate for offshore wave control: a review. Coast Eng J 44:127–147. https://doi.org/10.1142/S0578563402000470